Sangeeta Dhawan,[1] Ercument Dirice,[2] Rohit N. Kulkarni,[2] and Anil Bhushan[3]

CrossMark

Inhibition of TGF-β Signaling Promotes Human Pancreatic β-Cell Replication

SIGNAL TRANSDUCTION

Diabetes is associated with loss of functional pancreatic β-cells, and restoration of β-cells is a major goal for regenerative therapies. Endogenous regeneration of β-cells via β-cell replication has the potential to restore cellular mass; however, pharmacological agents that promote regeneration or expansion of endogenous β-cells have been elusive. The regenerative capacity of β-cells declines rapidly with age, due to accumulation of p16^{INK4a}, resulting in limited capacity for adult endocrine pancreas regeneration. Here, we show that transforming growth factor-β (TGF-β) signaling via Smad3 integrates with the trithorax complex to activate and maintain *Ink4a* expression to prevent β-cell replication. Importantly, inhibition of TGF-β signaling can result in repression of the *Ink4a/Arf* locus, resulting in increased β-cell replication in adult mice. Furthermore, small molecule inhibitors of the TGF-β pathway promote β-cell replication in human islets transplanted into NOD-*scid* IL-2Rg^{null} mice. These data reveal a novel role for TGF-β signaling in the regulation of the *Ink4a/Arf* locus and highlight the potential of using small molecule inhibitors of TGF-β signaling to promote human β-cell replication.

Replication of β-cells is the primary mechanism for maintenance and expansion of β-cell mass in response to changing insulin demands (1–4), and failure of such adaptive expansion can result in diabetes (5,6). Induction of p16^{INK4a} expression, a product of the *Ink4a/Arf* locus, is typical in adult tissues (7,8) and contributes to reduced self-renewal across mammalian tissues, including β-cells (9–11). This reflects in the reduced ability of the endocrine pancreas for adaptive expansion and regeneration (12,13). The *Ink4a/Arf* locus has also been linked with

type 2 diabetes in genome-wide association studies (14). Thus, manipulation of mechanisms that regulate the *Ink4a/Arf* locus could serve a tool for promoting adult β-cell replication.

Several studies, including ours, have shown that distinct repressive complexes of polycomb group proteins regulate β-cell replication during aging by epigenetically targeting the *Ink4a/Arf* locus (15,16). Polycomb repressive complex 2 (PRC2) contains histone H3K27 methyltransferase Ezh2 and marks the target chromatin with lysine 27 trimethylation of histone H3 (H3K27me3). This directs the recruitment of polycomb repressive complex 1 (PRC1; contains Bmi1 and ubiquitin ligase-Ring1B), leading to the ubiquitination of lysine 119 in histone H2 (H2AK119) (11,17). Together, these epigenetic modifications result in the repression of the *Ink4a/Arf* locus in juvenile β-cells to maintain replicative potential. The loss of polycomb complex binding in adult β-cells results in the recruitment of histone methyltransferase Mll1, which mediates trimethylation of lysine 4 in histone H3 (H43K4me3), an activating histone modification (15,16). In β-cells, Mll1 exists in a complex with histone H3K27me3 demethylase JmjD3, which removes the repressive H3K27me3 modifications (18). Together, the recruitment of the Mll1-JmjD3 complex leads to the induction of p16^{INK4a} expression (15,16,18), resulting in reduced β-cell replication. Our recent work shows that a combination of polycomb replenishment with loss of Mll1 complex binding can drive replication in adult β-cells (18).

Although recent work has unraveled cellular signals, such as platelet-derived growth factor that regulate the repression of p16^{INK4a} expression and β-cell self-renewal in young adults (19), the signals that mediate the induction

[1]Division of Endocrinology, Department of Medicine, University of California, Los Angeles, Los Angeles, CA
[2]Islet Cell and Regenerative Biology, Joslin Diabetes Center and Department of Medicine, Brigham and Women's Hospital, Harvard Medical School, Boston, MA
[3]Diabetes Center, University of California, San Francisco, San Francisco, CA

Corresponding author: Anil Bhushan, anil.bhushan@ucsf.edu.

of *Ink4a/Arf* locus in late adult life are not known. Here, we report that transforming growth factor-β (TGF-β) signaling induces *Ink4a* expression leading to replicative decline in β-cells through the recruitment of Smad3 as a part of the Mll1 complex. Smad3 is a downstream effector of the canonical TGF-β signaling and translocates to the nucleus upon its phosphorylation as a consequence of ligand binding to the TGF-β receptor (20). We demonstrate that inhibition of TGF-β signaling using small molecules can reduce the levels of p16^{INK4a} in a conserved fashion across cell types. Finally, we show that small molecule inhibitors of TGF-β signaling can be used to induce β-cell replication by lowering the cellular levels of p16^{INK4a}. Together, these studies provide a therapeutically relevant example of how cellular signals modulate β-cell replication via targeting epigenetic pathways.

RESEARCH DESIGN AND METHODS

Animal Maintenance
For the experiments involving mouse islets and mouse in vivo regeneration studies, the animals were maintained by mating wild-type males and females on a C57BL/6J background. Male NOD *Cg-Prkdc^{scid}Il2rg^{tm1Wjl}/SzJ* (NOD-*scid* IL-2Rg^{null} [NSG]) (denoted NOD-*scid*-γ or NSG) mice (8–10 weeks old) were used for human islet transplant experiments. All animal experiments were performed in accordance with National Institutes of Health policies on the use laboratory animals and approved by the Animal Research Committee of the Office for the Protection of Research Subjects at the University of California, Los Angeles, and Joslin Diabetes Center Institutional Animal Care and Use Committee protocols.

Animal Experiments
For experiments on the effect of TGF-β inhibitor on mouse β-cell replication in vivo, wild-type C57BL/6J mice (age 9 months) were divided into two groups (*n* = 9 per group) and injected intraperitoneally with a single dose of TGF-β inhibitor SB431542 (5 mg/kg body weight [BW]) or vehicle control (50% [v/v] DMSO), ensuring that the volume injected was kept up to 100 μL. Previous long-term studies have shown that the concentration of DMSO used as vehicle in these studies has no adverse effects on mouse health (21). Pancreata from these mice were harvested and processed for histology and analyzed for proliferation after 1 week (4). For human islet graft experiments, male NSG mice (*n* = 4) were used for experiments and grafted with human islets (1,000 islet equivalents) under the kidney capsule as previously described (22,23). One week after transplantation (when the islets developed vascular anastomosis), mice were injected intraperitoneally with vehicle or TGF-β inhibitor (5 mg/kg/BW, 50% [v/v] DMSO) twice weekly for 3 weeks. Four weeks after transplantation, mice were intraperitoneally injected with BrdU (Sigma-Aldrich, St. Louis, MO) (100 mg/kg/BW) for 3 days and killed 6 h after receiving the final BrdU injection. Blood was collected before and 2 and 4 weeks

after islets were grafted for the measurement of human insulin (Human Insulin ELISA Kit; Mercodia) and human C-peptide (C-Peptide ELISA Kit; Mercodia). In vivo glucose-stimulated insulin secretion (3 g/kg/BW, 20% dextrose) was performed at 3 weeks post-transplantation after overnight fasting. The graft-containing kidneys and pancreata were embedded in paraffin and prepared for histological analysis (24).

Cell Culture, Islet Isolation, and Culture-Inhibitor Treatments
Mouse embryonic fibroblasts (MEFs) were maintained on dishes coated with 0.2% porcine gelatin in DMEM-based medium containing 10% FBS at 37°C in a 5% CO_2 environment. Mouse islets were isolated using the Liberase/DNase enzyme mix (Roche Diagnostics) as previously described (25). In brief, the pancreas was inflated with the enzyme mix through the common bile duct and digested at 37°C. Islets were enriched by gradient and handpicked. Human islet samples from healthy adult organ donors without diabetes who died of acute trauma or anoxia were obtained from the Integrated Islet Distribution Program, as previously described (4). From 100 to 200 islets were cultured in a 35 mm × 10 mm easy-grip tissue culture dish (Falcon) in DMEM (CellGro) containing 10% FBS, supplemented with 11 mmol/L D-glucose (mouse islets) or 5 mmol/L D-glucose (human islets). For experiments involving the effect of TGF-β on cellular aging and proliferation, early-passage MEFs (passage 2 [P2]) in culture were supplemented with 5.0 ng/mL TGF-β (PeproTech) for 2 days (for proliferation assay) and for the indicated number for days (for growth curve), with daily change of culture medium. For experiments with TGF-β inhibitors, islets from old mice (8–12 months old) and late-passage MEFs (passage 9–12 [P9–12]) were cultured with one of the following TGF-β inhibitors, SB431542 (15 μmol/L; Sigma-Aldrich), SB505124 (5 μmol/L; Sigma-Aldrich), or SD208 (10 μmol/L; Sigma-Aldrich), or control small molecule phosphatidylinositide 3 kinase inhibitor LY294002 (10 μmol/L; Sigma-Aldrich) for 3 days for replication analysis and the indicated number of days for cell growth curves, with daily change of culture medium. For cell growth measurements, the number of cells was measured at indicated times and after indicated treatments by using a hemocytometer and plotted as a function of time. Human islets from cadaveric donors were cultured for 4 days with SB431542 (40 μmol/L; Sigma-Aldrich) or vehicle control (DMSO) and then harvested for replication analysis. Western blots with the indicated antibodies were performed, as previously described (25).

Immunofluorescence Staining and Morphometric Analyses
A standard immunofluorescence staining protocol was used to detect various protein markers in mouse pancreatic islet sections (4). Cultured islets were harvested, fixed in 4% paraformaldehyde, embedded in histogel matrix, and processed according to the above protocol. MEFs

were fixed as monolayers in culture (on gelatin-coated plastic ware) for 20–30 min at room-temperature with the BD Cytofix/Cytoperm solution (BD Pharmingen) and washed thoroughly three times with 1× BD Perm/Wash buffer, followed by permeabilization at room temperature in the same buffer. Primary antibodies were diluted in the blocking solution (3% BSA in Tris-buffered saline with Tween) at the following dilutions: guinea pig anti-insulin (diluted 1:400; Dako), mouse anti-Ki67 (diluted 1:50; BD Pharmingen), mouse anti-BrdU (diluted 1:2; GE Healthcare/ Amersham RPN-202); anti-phosphorylated histone H3 (diluted 1:200; Millipore pHH3), rabbit anti-Pdx1 (diluted 1:200; Millipore), and mouse anti-p16 (diluted 1:400; Santa Cruz sc-1661). Donkey- and goat-derived secondary antibodies conjugated to FITC or Cy3 were diluted 1:500 (Jackson ImmunoResearch Laboratories).

Slides were viewed using a Leica DM6000 microscope, and images were acquired using Openlab software (Improvision). The proliferation index was calculated using Ki67, BrdU, or pHH3 staining as a measure of cell proliferation by costaining the islet sections for Ki67 (or BrdU or pHH3) and insulin or Pdx1 for β-cells and by costaining for Ki67 with the nuclear marker DAPI for MEFs. β-Cell area was evaluated by point-counting morphometry on immuno-fluorescence-stained pancreatic sections. Cell death was detected by TUNEL assay (ApopTag S7100; Millipore). At least 2,000–3,000 β-cell nuclei were counted per animal.

Immunoprecipitation and Western Blotting
As previously published, 2.5 mg anti-Mll1 antibody (Millipore 05-765) or control IgG was used for each immunoprecipitation on MEF lysates. Briefly, antibodies were bound to Protein G Sepharose (Millipore) for 2–3 h and incubated with MEF extracts prepared overnight at 4°C on a rotator. The immunoprecipitates were analyzed by Western blotting with antibodies against JmjD3 (Millipore; 07-1434), Smad3 antibody (Bethyl Laboratories; A300-109A), and control Dnmt3a (Imgenex; IMG-268A). Samples for Western blotting were lysed in cell dissociation buffer (Invitrogen) supplemented with protease inhibitors cocktail (Calbiochem), as described. The following primary antibodies were used: mouse anti-p16 (Santa Cruz; sc-1661), mouse anti-Smad3 (BD Biosciences; 610842), rabbit anti-phosphorylated (p)Smad3 (07-1389), and mouse anti–β-tubulin (Sigma-Aldrich; T8328). Each Western blot is a representative from three independent experiments using different sample preparations.

Chromatin Immunoprecipitation Analysis
Chromatin immunoprecipitation (ChIP) was performed as previously reported (26), with minor modifications. The islets (150–200 islets per group, made into single-cell suspension) or MEFs (1×10^5 cells) were treated with 1% paraformaldehyde at room temperature for 20 min to crosslink the DNA with bound proteins. Formaldehyde was quenched by adding glycine to a final concentration of 125 mmol/L, followed by cell lysis in 100 μL lysis buffer consisting of 50 mmol/L Tris HCl (pH 8.0), 10 mmol/L EDTA, 1% SDS, supplemented with 1× complete proteinase inhibitors (Calbiochem), and sonicated to yield DNA fragments with an average size of 500 bp using Bioruptor (Diagenode). A total of 2.5 μg antibody was bound to 20 μL Protein-A/G Dynabeads (Invitrogen), depending on the antibody isotype, for 2 h at 4°C with agitation. The following antibodies were used: anti–3me-H3K27 (Millipore; 07-449), anti–H3K4 me3 (Cell Signaling; 9751S), anti-JmjD3 (Millipore; 07-1534), anti-MLL1 (Millipore; 05-765), and anti-Smad3 (BD Biosciences; 610842), or normal mouse IgG as a control. One-fourth fraction of the sonicated chromatin was incubated overnight at 4°C with the antibody-bead complexes in total volume of 200 μL in RIPA buffer containing 10 mmol/L Tris HCl (pH 8.0), 140 mmol/L NaCl, 1 mmol/L EDTA, 1% Triton X-100, 0.1% SDS, and 0.1% Na-deoxycholate supplemented with 1× complete proteinase inhibitors. After washing four times with radioimmunoprecipitation assay buffer and twice with Tris-EDTA buffer, chromatin was eluted, followed by reverse crosslinking at 68°C for 4 h with vigorous agitation in the presence of Proteinase K (Sigma-Aldrich). The DNA fragments were then purified using phenol-chloroform extraction and ethanol precipitation. The resulting DNA was quantified and served as a template for the real-time PCR reactions, performed using ABI7900HT (Applied Biosystems), with 1× Fast SYBR Green Mix (Applied Biosystems). The DNA enrichment after ChIP was estimated as percentage bound-to-input ratio determined by real-time PCR. The primers used to amplify the *Ink4a/Arf* locus have been described before (11,16).

Statistical Methods
All data are expressed as mean ± SE. Mean and SEM values were calculated from at least triplicates of a representative experiment. The statistical significance of differences was measured by unpaired Student t test for experiments with two groups and a continuous outcome or by one-way ANOVA for repeat measures. A P value of <0.05 indicated statistical significance.

RESULTS

TGF-β Signaling Induces the Expression of p16^{INK4a} via Recruitment of the Mll1 Complex
To understand the mechanisms that mediate the recruitment of the Mll1 complex to the *Ink4a/Arf* locus during replicative decline, we first used the MEFs model. P2 MEFs are characterized by low p16^{INK4a} and high proliferation, whereas P9–12 MEFs accumulate p16^{INK4a}, resulting in reduced proliferation (11,18). Coimmunoprecipitation of Mll1 complex components, followed by mass spectrometry, suggested that the Mll1 complex interacted with the TGF-β signaling pathway effectors (data not shown). Therefore, we assessed the interaction between the Mll1 complex and TGF-β pathway using anti-Mll1 antibody immunoprecipitate from P9 MEFs. Western blotting using the Smad3 antibody

revealed that Smad3 interacts with Mll1 (Fig. 1A and B). Using ChIPs, we compared the binding of Smad3 to the *Ink4a/Arf* locus in P2 and P9 MEFs. Smad3 was recruited to the *Ink4a/Arf* locus in the P9 MEFs, suggesting a correlation between Smad3 binding and induction of p16^{INK4a} (Fig. 1C). This was further confirmed by treatment of P2 MEFs with TGF-β, which resulted in recruitment of Smad3 to the *Ink4a/Arf* locus, along with Mll1 and JmjD3 (Fig. 1D and Supplementary Fig. 1A), resulting in increased H3K4me3 (activating histone modification) and reduced H3K27me3 (repressive modification) levels (Supplementary Fig. 1B and C). This resulted in a significant reduction in the proliferation of P2 MEFs treated with TGF-β, due to the accumulation of p16^{INK4a} (Fig. 1E–G and Supplementary Fig. 1D), which was associated with increased levels of pSmad3 (Supplementary Fig. 1E). Taken

together, these observations suggested a novel role for TGF-β in the transcriptional regulation of *Ink4a/Arf* locus.

Inhibition of TGF-β Signaling Disrupts the Association of Smad3 With the *Ink4a/Arf* Locus to Promote Proliferation in P9 MEFs

To confirm if TGF-β signaling is associated with reduced proliferative potential through induction of p16^{INK4a} expression, we treated P9 MEFs with SB431542 (27), a well-characterized inhibitor of TGF-β signaling that blocks phosphorylation of Smad3 via the ALK5 receptor. Treatment of P9 MEFs with SB431542 reduced the association of Smad3 (Fig. 2A), Mll1, and JmjD3 to the *Ink4a/Arf* locus (Fig. 2B), resulting in reduced H3K4me3 and increased H3K27me3 levels (Supplementary Fig. 2A and B). This led to reduced levels of p16^{INK4a} and increased
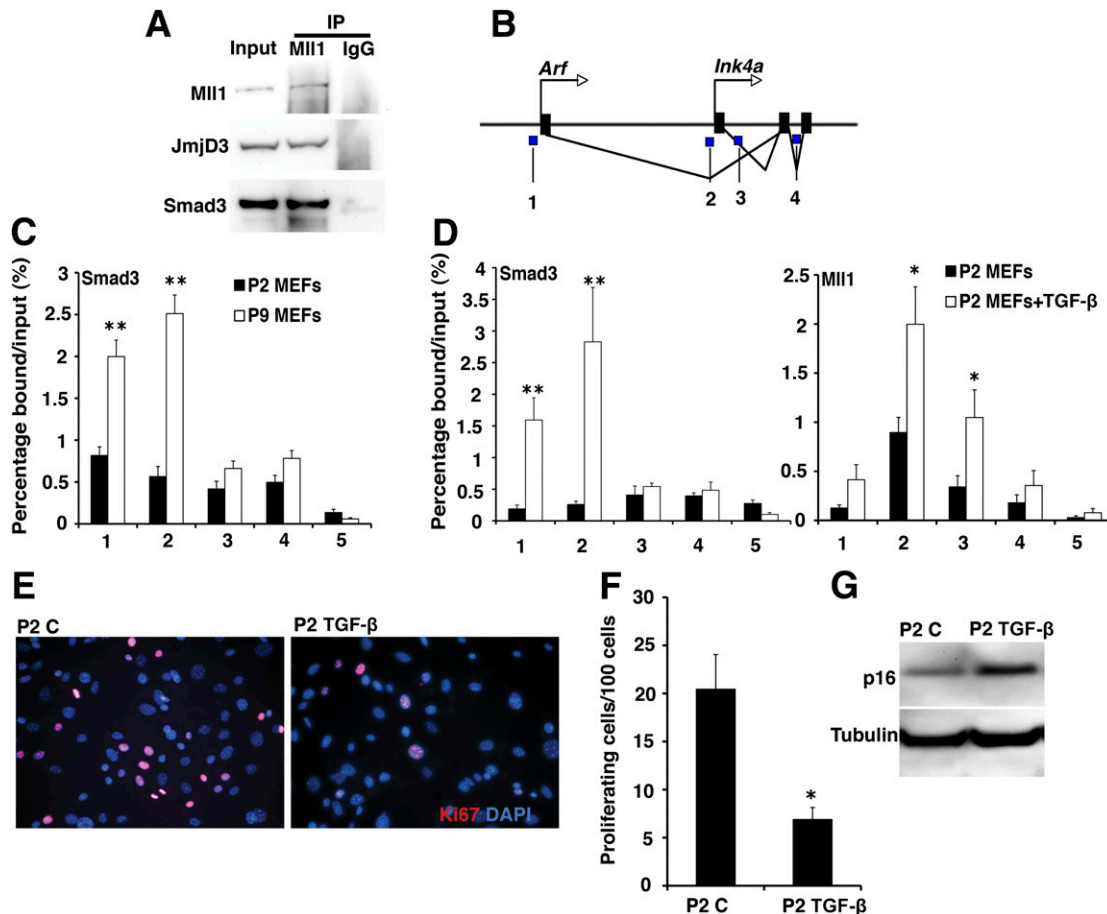

Figure 1—*A*: Coimmunoprecipitation analysis examining the interaction of Mll1 complex with Smad3. Cell extracts from P9 MEFs were used as input for immunoprecipitation (IP) with anti-Mll1 antibody (or control IgG) and analyzed by immunoblotting with Mll1, JmjD3, and Smad3 antibodies. Bmi1 antibody was used as a negative control. Representative experiment from *n* = 3. *B*: Schematic representation of the *Ink4a/Arf* locus, with blue regions marked 1–4 indicating the amplified regions in the ChIP studies. *C*: ChIP analysis comparing the recruitment of Smad3 (using a Smad3 antibody) to the *Ink4a/Arf* locus, in P2 and P9 MEFs (*n* = 3). 1–4 indicate the amplified regions at the *Ink4a/Arf* locus, and 5 indicates binding for the negative control corresponding to exon 2 in the *Hox*^{13}C locus (43). *D*: ChIP analyses comparing the recruitment of Smad3 and Mll1 to the *Ink4a/Arf* locus, in P2 MEFs treated with TGF-β or vehicle control (*n* = 3). 1–5 indicate the amplified regions, with 5 being the negative control. Immunofluorescence (*E*) and quantification (*F*) for proliferation in P2 MEFs treated with TGF-β or vehicle control (C), using immunostaining with Ki67 antibody (red). DAPI (blue) is a nuclear counterstain. Representative experiment from *n* = 3. *G*: Western blotting for p16 and β-tubulin in cell extracts from P2 MEFs treated with TGF-β or vehicle control (C) (*n* = 3). Error bars indicate ± SEM. *P* values were determined by unpaired Student *t* test. *P < 0.05; **P < 0.01.
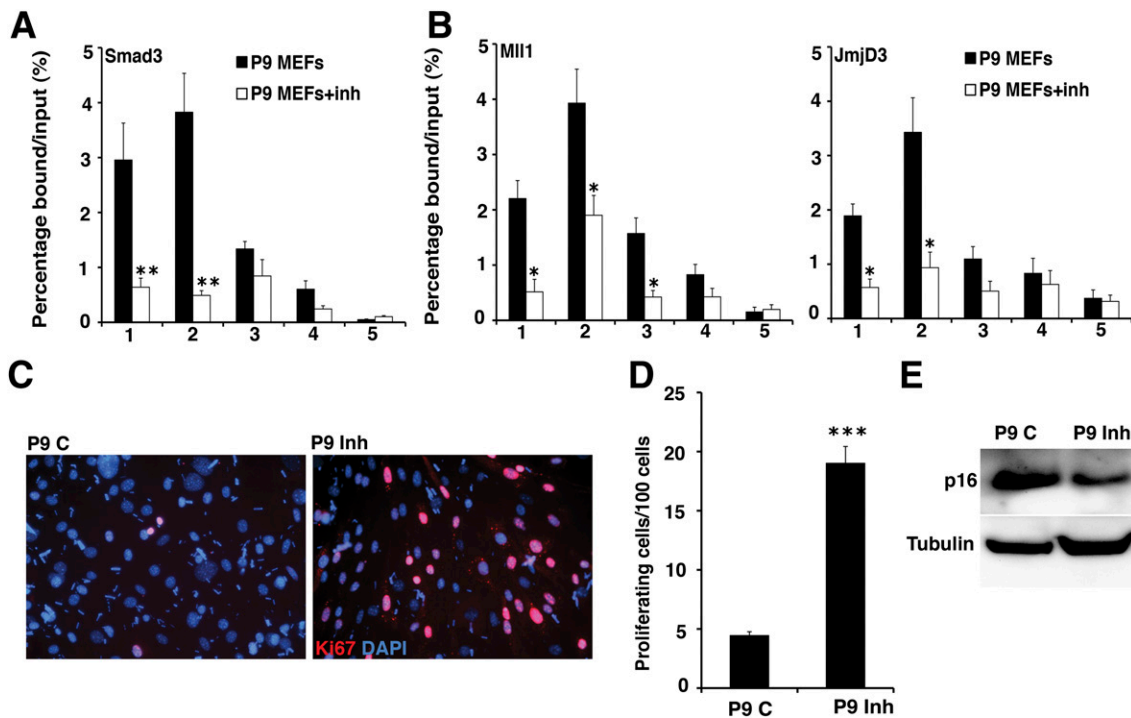
Figure 2—*A*: ChIP analysis comparing the recruitment of Smad3 to the *Ink4a/Arf* locus, in P9 MEFs in the presence (MEFs+inh) or absence of TGF-β inhibitor (*n* = 3). 1–5 indicate the amplified regions, with 5 being the negative control. *B*: ChIP analyses comparing the recruitment of Mll1 and JmjD3 to the *Ink4a/Arf* locus, in P9 MEFs treated with TGF-β inhibitor (MEFs+inh) or vehicle control (*n* = 3). 1–5 indicate the amplified regions, with 5 being the negative control. Immunofluorescence (*C*) and quantification (*D*) for proliferation in P9 MEFs treated with TGF-β inhibitor (Inh) or vehicle control (C), using immunostaining with Ki67 antibody (red), counterstained with DAPI (blue) to mark the nuclei (*n* = 3). *E*: Western blotting for p16 and β-tubulin in cell extracts from P9 MEFs treated with TGF-β inhibitor (Inh) or vehicle control (C). Representative experiment from *n* = 3. Error bars indicate ± SEM. *P* values were determined by unpaired Student *t* test. **P* < 0.05; ***P* < 0.01; ****P* < 0.001.

proliferation of P9 MEFs treated with SB431542 (Fig. 2C–E and Supplementary Fig. 2C). This suggested that indeed the decline in proliferative potential due to p16INK4a accumulation in P9 MEFs is mediated by TGF-β signaling. To test if the effect of TGF-β inhibitor on induction of proliferation was reversible, we cultured P9 MEFs in the presence of SB431542, followed by inhibitor withdrawal after 4 days of treatment. Withdrawal of SB431542 resulted in a decline in the proliferation compared with P9 MEFs that were continuously maintained in the presence of inhibitor (Supplementary Fig. 2D), suggesting a transient effect of TGF-β inhibitor on increasing proliferation.

TGF-β Inhibition Can Induce β-Cell Replication in Islets From Adult Mice by Reducing p16INK4a Levels

On the basis of the observations in MEFs, we examined the effect of TGF-β signaling on regulation of the *Ink4a/Arf* locus in islets. ChIP analysis showed increased recruitment of Smad3 to the *Ink4a/Arf* locus in islets from 9-month-old mice compared with islets from younger juvenile mice (Fig. 3A). Treatment of pancreatic islets isolated from 9- to 12-month-old mice with SB431542 resulted in reduced binding of Smad3, Mll1, and JmjD3 complex to the *Ink4a/Arf* locus (Fig. 3B and Supplementary Fig. 3A), concomitant with increased H3K27me3 and reduced H3K4me3 levels at

the *Ink4a/Arf* locus (Supplementary Fig. 3B and C). We then cultured the islets from adult mice (aged 9–12 months) with TGF-β inhibitor or vehicle control. The β-cells (marked by Pdx1) from islets treated with SB431542 showed increased replication (Fig. 3C and D) due to reduced levels of p16INK4a in these islets (Fig. 3E). The specific effect of inhibition of TGF-β signaling on β-cell replication was further confirmed by treatment of islets from aged mice with two other known TGF-β signaling inhibitors, namely SB505124 and SD208, which showed a similar effect on increased replication, whereas LY294002, a phosphatidylinositide 3 kinase inhibitor used as a control, did not result in any significant increase in replication (Supplementary Fig. 3D and E). Thus, treatment with small molecule inhibitors of TGF-β signaling can promote β-cell replication in islets from adult mice that typically exhibit resistance to induction of replication and regeneration (13).

Treatment of Mice With TGF-β Inhibitor Stimulates β-Cell Replication

To establish whether treatment with TGF-β inhibitor can stimulate β-cell regeneration in adult mice in vivo, we injected 9-month-old mice intraperitoneally with one dose of SB431542 or vehicle control (*n* = 9 per group). The pancreas was harvested after 1 week, and coimmunostaining of
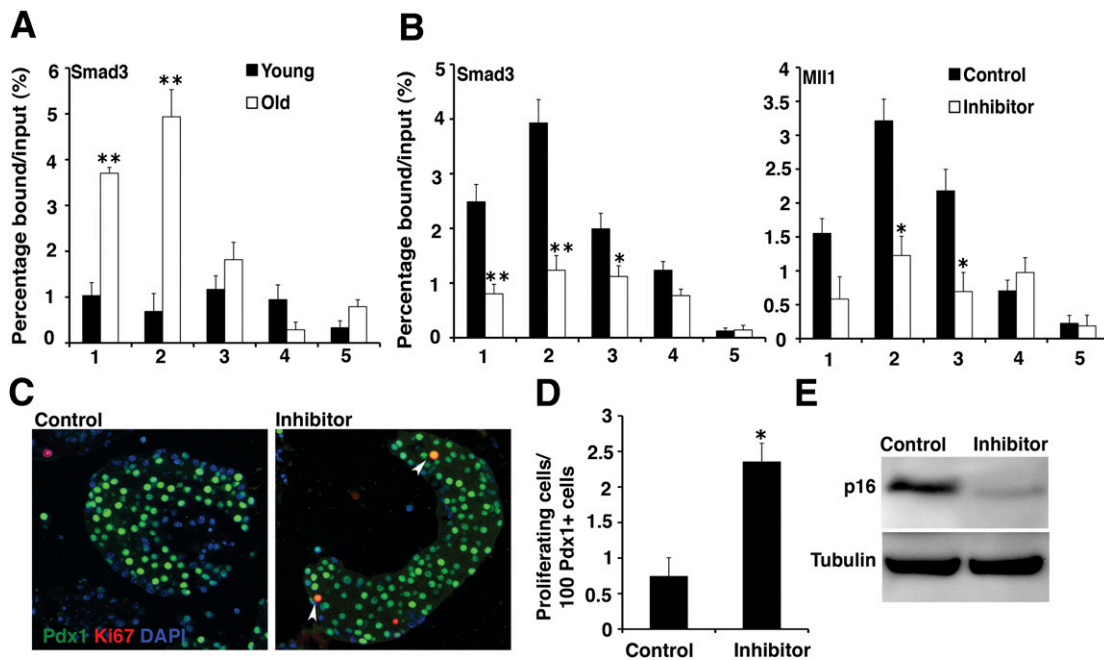
Figure 3—A: ChIP analysis comparing the recruitment of Smad3 to the *Ink4a/Arf* locus in islets from young (2.5 months) or old (9 months) mice ($n = 3$). 1–5 indicate the amplified regions, with 5 being the negative control. B: ChIP analyses comparing the binding of Smad3 and Mll1 in islets from old (9 months) mice, treated with TGF-β inhibitor SB431542 (inhibitor) or vehicle control ($n = 3$). 1–5 indicate the amplified regions, with 5 being the negative control. Immunohistochemistry (C) and quantification (D) for proliferation of β-cells in islets from 9-month-old mice treated with TGF-β inhibitor or vehicle control, using immunostaining with Ki67 antibody (red) and β-cell marker Pdx1 (green). Arrowheads mark Ki67 Pdx1 double-positive cells. Counterstain DAPI (blue) marks the nuclei ($n = 3$). E: Western blotting for p16 and β-tubulin in extracts from islets from 9-month-old mice treated with TGF-β inhibitor or vehicle control. Representative experiment from $n = 3$. Error bars indicate ± SEM. P values were determined by unpaired Student t test. *$P < 0.05$; **$P < 0.01$.

pancreatic sections for Ki67 and insulin showed increased β-cell replication of SB431542 in treated mice compared with control mice (Fig. 4A and B). The increase in β-cell proliferation was accompanied by a reduction in $p16^{INK4a}$ levels in islets (Fig. 4C). We previously showed that polycomb regulation of $p16^{INK4a}$-dependent changes that limits β-cell replication is conserved in human islets (18). We then examined whether β-cell replication can be induced in human islets by inhibition of the TGF-β pathway. Treatment of human islets (from donors aged 40–60) with SB431542 resulted in increased β-cell replication compared with vehicle control (Fig. 4D). The increased replication in the inhibitor-treated group correlated with reduced binding of Mll1 and Smad3 at the *Ink4a/Arf* locus (Supplementary Fig. 4A and B). Thus, inhibition of TGF-β signaling improves β-cell replication in both mice and humans.

TGF-β Inhibitor Stimulates β-Cell Replication in Grafted Human Islets

To further evaluate the stimulatory effect of TGF-β inhibitor on human β-cell proliferation, we used a model in which 1,000 human islet equivalents were transplanted under the kidney capsule of male NSG mice (28). One week after transplantation, mice receiving human islet grafts were treated with the TGF-β inhibitor (5 mg/kg/BW, 50% [v/v] DMSO) or vehicle control (DMSO), and sham-operated mice did not receive any treatment. Graft survival and functionality was examined by insulin secretory responses to glucose, using an ultrasensitive human insulin ELISA assay, in mice that received human islets (Supplementary Fig. 5A). Detection of human insulin and C-peptide levels in the circulation 2 and 4 weeks after transplantation indicated the presence of viable human islet grafts (Supplementary Fig. 5B and C). Immunohistochemical analysis of human islet graft–bearing kidney sections showed a ~10-fold ($P < 0.05$) increase in BrdU incorporation in the TGF-β inhibitor–treated group, indicating a transition from G1 to S-phase of the cell cycle (Fig. 5A–G and Supplementary Fig. 5D). The enhanced mitosis was confirmed by an approximately fourfold ($P < 0.05$) increase in Ki67+ β-cells in the treated group (Fig. 5H and Supplementary Fig. 5E), and an augmentation in pHH3+ β-cells suggesting progression into the G2/M phases ($P = 0.07$) (Fig. 5I). In untreated mice, the rate of human β-cell replication was virtually undetectable, consistent with previous findings under similar conditions (22,23). Analysis of $p16^{INK4a}$ expression in these graft samples by immunohistochemistry showed reduced $p16^{INK4a}$ levels upon treatment with TGF-β inhibitor, consistent with our earlier observations in mice (Fig. 5J). Furthermore, examination of endogenous mouse pancreas of both groups demonstrated significantly lower β-cell apoptosis ($P = 0.005$) in the TGF-β inhibitor–treated group compared with control
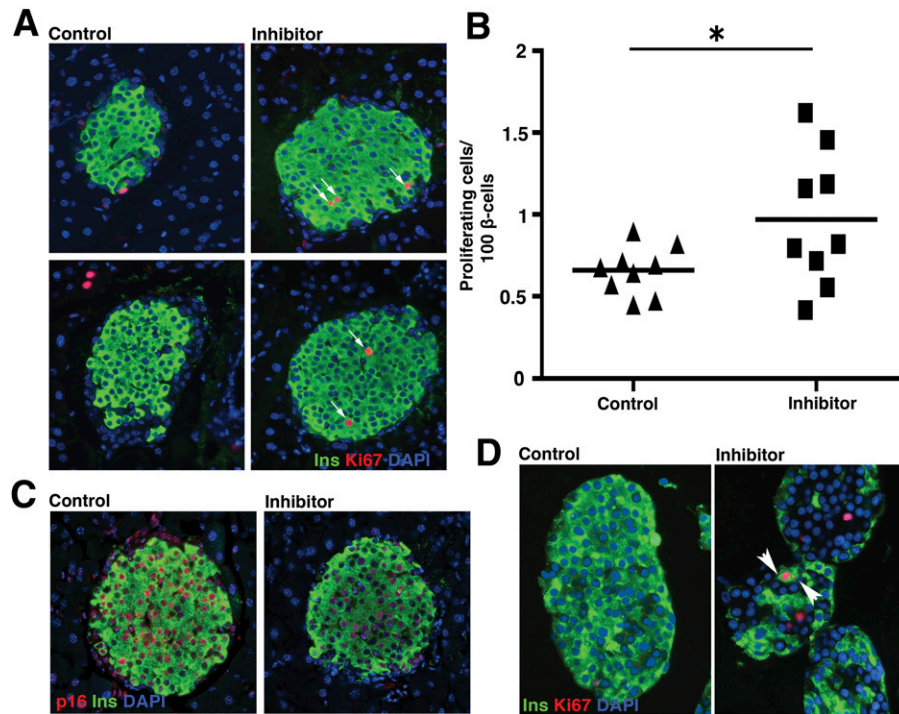
Figure 4—Immunohistochemistry (*A*) and quantification (*B*) for proliferation of β-cells in pancreatic sections from 9-month-old mice injected intraperitoneally with TGF-β inhibitor or vehicle control, using immunostaining with Ki67 antibody (red) and insulin (green), along with nuclear counterstain DAPI (blue). Arrows mark the proliferating β-cells, labeled by Ki67 and insulin (*n* = 9). *C*: Immunohistochemistry for p16[INK4a] levels in pancreatic sections from 9-month-old mice injected intraperitoneally with TGF-β inhibitor or vehicle control, using immunostaining with p16[INK4a] antibody (red) and insulin (green), along with DAPI (blue). Representative experiment from *n* = 9. *D*: Immunohistochemistry for Ki67 (red), along with insulin (green) and DAPI (blue) for proliferation of β-cells in human islets treated with TGF-β inhibitor or vehicle control. Arrowheads mark proliferating β-cells. Representative experiment from *n* = 3. Error bars indicate ± SEM. *P* values were determined by unpaired Student *t* test. *$P < 0.05$.

mice (Supplementary Fig. 6*A*). Despite the increased β-cell replication upon TGF-β inhibitor treatment of mouse islets and human islet grafts, and decreased β-cell apoptosis in mouse islets, the β-cell area, and islet density were not different between groups (Supplementary Fig. 6*B* and *C*). Thus, treatment with TGF-β inhibitor can be effectively used to promote replication of human β-cells.

In parallel, we evaluated endogenous islets of the NSG mice that received the TGF-β inhibitor. Consistent with our previous data in independent studies (Fig. 4*B*), the group that received TGF-β inhibitors exhibited a significant increase in three different proliferation markers, namely, BrdU (0.27% ± 0.06 vs. 0.06% ± 0.02, *P* = 0.028), Ki67 (0.2% ± 0.03 vs. 0.09% ± 0.01, *P* = 0.047), and pHH3 (0.12% ± 0.02 vs. 0.03% ± 0.02, *P* = 0.039) (Fig. 6*A–C*) in the pancreatic β-cells. Similar to human islet grafts without treatment, β-cell replication in untreated and sham-operated mice was minimal. In addition, the pancreatic β-cell proliferation was accompanied by a reduction in p16[INK4a] levels in the islets (Fig. 6*D*). Taken together, our studies suggest that TGF-β signaling induces age-related accumulation of p16[INK4a], leading to replicative decline and that treatment with TGF-β inhibitor can effectively induce replication in both mouse and human β-cells.

DISCUSSION

Previous work on TGF-β signaling has largely focused on pancreatic development and islet homeostasis and function (29–34). Here, we delineate the mechanism by which TGF-β signaling controls replicative senescence across cell types, including mouse and human β-cells, by regulating the *Ink4a/Arf* locus. More importantly, we have used small molecule inhibitors of the TGF-β pathway to stimulate mouse and human β-cell replication in vitro and in vivo. TGF-β signaling is known to inhibit cell proliferation, and disruptions in TGF-β signaling are associated with overcoming senescence (35–37), as reviewed by Padua and Massagué (38). It is important to note that we observed a two- to threefold increase in β-cell replication with TGF-β inhibitors, which is comparable to the rates of replication observed during physiological β-cell mass expansion.

TGF-β1, -2, and -3 ligands are endogenously expressed within the human pancreas, not just in islets, but also in ducts as well as in the acini (3). This suggests that TGF-β ligands may work in both autocrine and paracrine fashion in the pancreas. TGF-β1 levels have been reported to increase with age in circulation as well as within several tissues (27,28). TGF-β signaling has been shown to be a critical signal in pancreatic development (39). Loss of
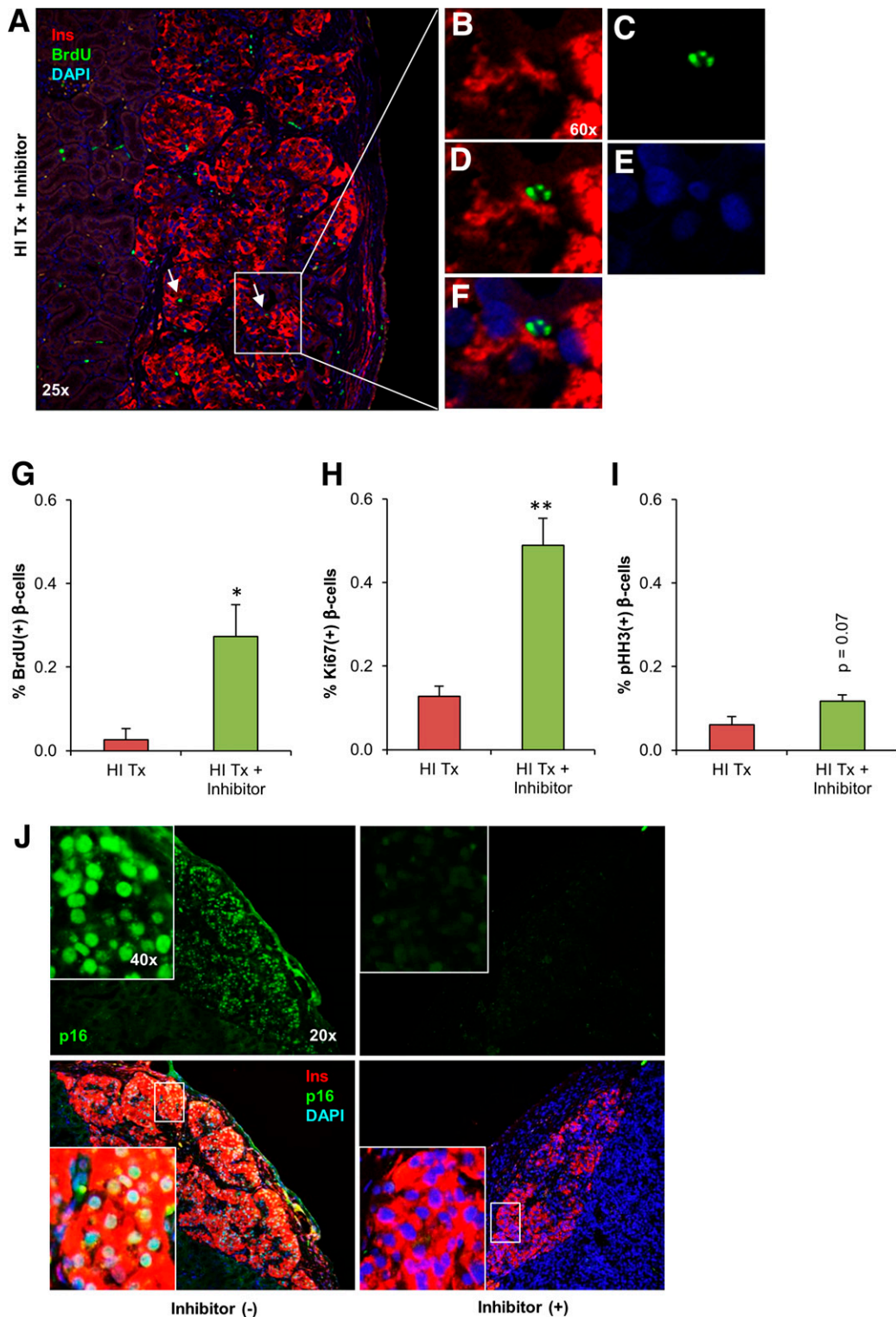
Figure 5—*A–F*: Confocal microscopy view of kidney sections derived from human islets (HI) transplanted (Tx) under the kidney capsule and treated with TGF-β inhibitor. Magnified area highlighted from *A* (right white box) shows imaging of insulin (red) (*B*, *D* and *F*), BrdU antibody (green) (*C*, *D*, and *F*), and DAPI (blue) (*E* and *F*). Arrows mark proliferating β-cells. Images (original magnification ×60) show each immunofluorescent staining separately (indicating nuclear gap for replicating β-cell surrounded by insulin) for the proliferating β-cells. Original magnification ×25 and ×60. Representative experiment from *n* = 4. Quantification of proliferating β-cells for BrdU/insulin (*G*), Ki67/insulin (*H*), and pHH3/insulin double-positive cells (*I*) from human islet–grafted and TGF-β inhibitor–treated groups. Between 1,000 and 2,000 β-cells were counted in each section (*n* = 4). *J*: Immunohistochemistry for p16INK4a in human islet–grafted kidney sections treated with or without TGF-β inhibitor, using insulin (red), p16 (green), and DAPI (blue). Representative experiment from *n* = 4. Error bars indicate ± SEM. *P* values were determined by unpaired Student *t* test. **P* < 0.05; ***P* < 0.01.
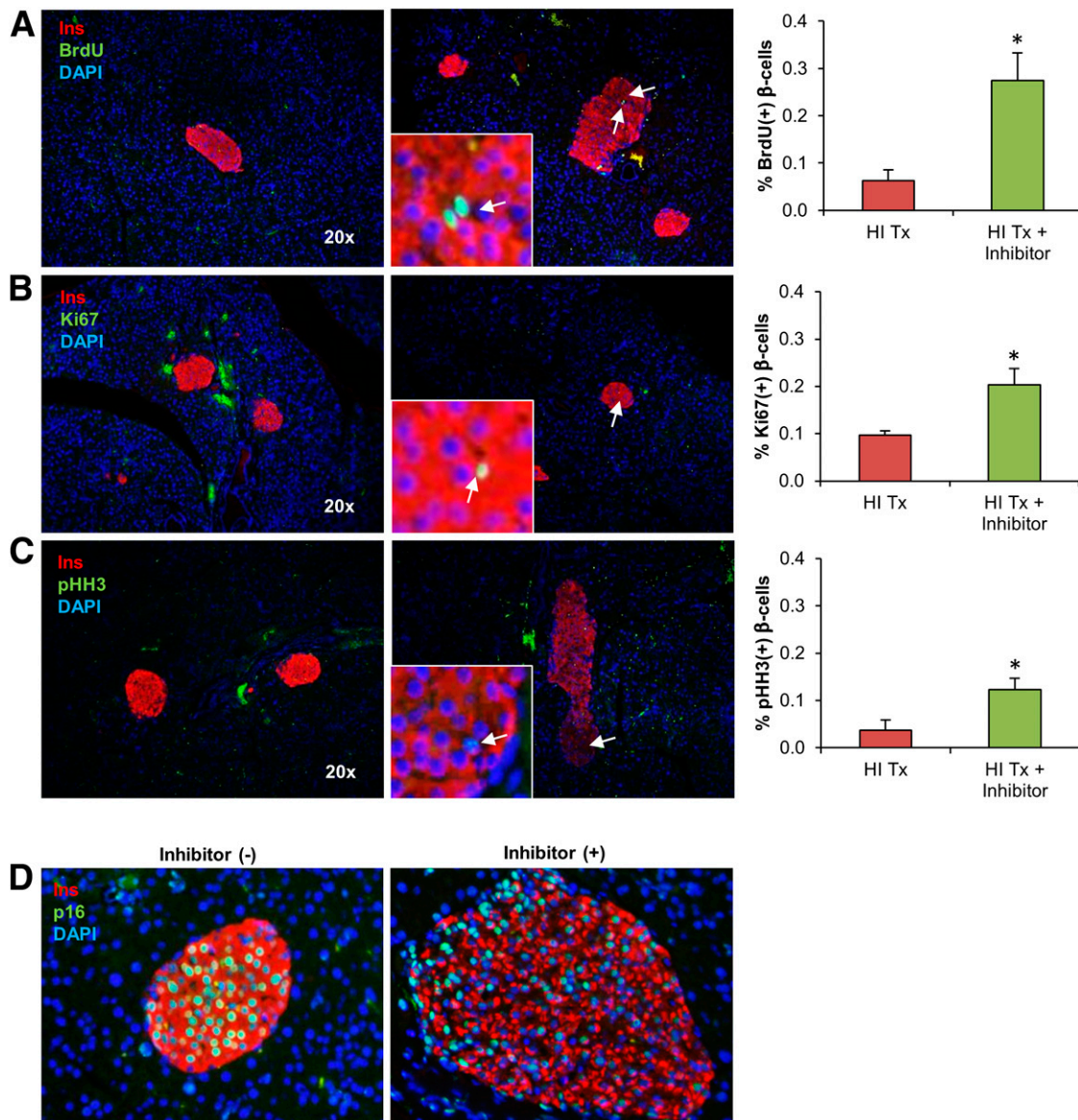
Figure 6—A–C: Immunohistochemistry and quantification for proliferating β-cells in pancreatic sections of human islet graft–bearing mice. Immunoflourescent staining for proliferation markers BrdU (A), Ki67 (B), and pHH3 (C). All proliferation markers are shown in green, insulin in red, and nuclear staining in blue. Arrows mark proliferating β-cells. Representative experiment from n = 4. D: Immunohistochemistry for p16INK4a in pancreatic section from human islet–grafted recipients, treated with or without TGF-β inhibitor, using insulin (red), p16 (green), and DAPI (blue). Representative experiment from n = 4. Error bars indicate ± SEM. P values were determined by unpaired Student t test. HI, human islet; Tx, transplants. *P < 0.05.

TGF-β type II receptor shows an increase in endocrine precursors and proliferating endocrine cells, suggesting that TGF-β signaling modulates the growth and differentiation of endocrine progenitors (40).

Disruptions in the canonical TGF-β signaling in the exocrine tissue result in islet hypertrophy (31), thus suggesting a role for TGF-β in regulating β-cell proliferation and islet homeostasis. Transient loss of Smad7 in the islets, using an inducible loss of function model, resulted in islet enlargement (32). More recently, genetic loss of Smad2 and -3 has been reported to result in a more robust proliferative response upon β-cell loss (29).

Another study showed loss of Smad2 induced islet hyperplasia and impaired insulin secretion (30). Studies using combined pan-pancreatic knockdown of TGF-β receptors I and II have also implicated TGF-β signaling in the regulation of β-cell proliferation (33). However, most of such work examining the TGF-β signaling on β-cell proliferation has been performed in the context of adaptive expansion in permissive age windows. Our work is the first to identify a key role for TGF-β signaling in age-dependent proliferative decline in pancreatic β-cells and to also establish a mechanism of cell cycle control via the INK4a locus.

TGF-β has been reported to stimulate insulin secretion (41), insulin gene transcription, and islet function (34). Further, TGF-β has been recently reported to have a protective effect on islet grafts in the murine models (40). Also, another recent study shows that inhibition of TGF-β signaling can reverse β-cell dedifferentiation in diabetes, suggesting an effect on function (42). These studies raise the possibility that treatment with TGF-β inhibitor may promote islet function and islet graft survival. In our studies using human islet grafts in humanized mice, however, the control and inhibitor-treated mice both showed comparable graft survival and human insulin and C-peptide secretion profiles. Considering *Ink4a* repression by polycomb group proteins is a well-conserved mechanism across cell types, additional work that addresses targeting of the small molecule inhibitors of the TGF-β signaling to the islet β-cells is warranted. Our study for the first time shows the connection between TGF-β signaling and p16^{Ink4a}-dependent replicative senescence in β-cells, thus providing a mechanistic insight into the age-dependent decline of β-cell replication. The experiments presented here establish a novel link between TGF-β signaling and the epigenetic regulation of β-cell replicative potential. These data provide an example of a pharmacological agent that can promote the replication of human β-cells with translational therapeutic potential to restore functional β-cell mass in patients with diabetes.

References

1. Dor Y, Brown J, Martinez OI, Melton DA. Adult pancreatic beta-cells are formed by self-duplication rather than stem-cell differentiation. Nature 2004;429: 41–46

2. Georgia S, Bhushan A. Beta cell replication is the primary mechanism for maintaining postnatal beta cell mass. J Clin Invest 2004;114:963–968

3. Yamanaka Y, Friess H, Büchler M, Beger HG, Gold LI, Korc M. Synthesis and expression of transforming growth factor beta-1, beta-2, and beta-3 in the endocrine and exocrine pancreas. Diabetes 1993;42:746–756

4. Zhong L, Georgia S, Tschen SI, Nakayama K, Nakayama K, Bhushan A. Essential role of Skp2-mediated p27 degradation in growth and adaptive expansion of pancreatic beta cells. J Clin Invest 2007;117:2869–2876

5. Kulkarni RN, Jhala US, Winnay JN, Krajewski S, Montminy M, Kahn CR. PDX-1 haploinsufficiency limits the compensatory islet hyperplasia that occurs in response to insulin resistance. J Clin Invest 2004;114:828–836

6. Okamoto H, Hribal ML, Lin HV, Bennett WR, Ward A, Accili D. Role of the forkhead protein FoxO1 in beta cell compensation to insulin resistance. J Clin Invest 2006;116:775–782

7. Nielsen GP, Stemmer-Rachamimov AO, Shaw J, Roy JE, Koh J, Louis DN. Immunohistochemical survey of p16INK4A expression in normal human adult and infant tissues. Lab Invest 1999;79:1137–1143

8. Krishnamurthy J, Torrice C, Ramsey MR, et al. Ink4a/Arf expression is a biomarker of aging. J Clin Invest 2004;114:1299–1307

9. Krishnamurthy J, Ramsey MR, Ligon KL, et al. p16INK4a induces an age-dependent decline in islet regenerative potential. Nature 2006;443:453–457

10. Kim WY, Sharpless NE. The regulation of INK4/ARF in cancer and aging. Cell 2006;127:265–275

11. Bracken AP, Kleine-Kohlbrecher D, Dietrich N, et al. The Polycomb group proteins bind throughout the INK4A-ARF locus and are disassociated in senescent cells. Genes Dev 2007;21:525–530

12. Rankin MM, Kushner JA. Adaptive beta-cell proliferation is severely restricted with advanced age. Diabetes 2009;58:1365–1372

13. Tschen SI, Dhawan S, Gurlo T, Bhushan A. Age-dependent decline in beta-cell proliferation restricts the capacity of beta-cell regeneration in mice. Diabetes 2009;58:1312–1320

14. Doria A, Patti ME, Kahn CR. The emerging genetic architecture of type 2 diabetes. Cell Metab 2008;8:186–200

15. Chen H, Gu X, Su IH, et al. Polycomb protein Ezh2 regulates pancreatic beta-cell Ink4a/Arf expression and regeneration in diabetes mellitus. Genes Dev 2009;23:975–985

16. Dhawan S, Tschen SI, Bhushan A. Bmi-1 regulates the Ink4a/Arf locus to control pancreatic beta-cell proliferation. Genes Dev 2009;23:906–911

17. Kotake Y, Cao R, Viatour P, Sage J, Zhang Y, Xiong Y. pRB family proteins are required for H3K27 trimethylation and Polycomb repression complexes binding to and silencing p16INK4alpha tumor suppressor gene. Genes Dev 2007; 21:49–54

18. Zhou JX, Dhawan S, Fu H, et al. Combined modulation of polycomb and trithorax genes rejuvenates β cell replication. J Clin Invest 2013;123:4849–4858

19. Chen H, Gu X, Liu Y, et al. PDGF signalling controls age-dependent proliferation in pancreatic β-cells. Nature 2011;478:349–355

20. Massagué J. TGF-β signaling in development and disease. FEBS Lett 2012; 586:1833

21. Kramer K, Van Acker SA, Grimbergen JA, van den Berg DJ, Van der Vijgh WJ, Bast A. Effect of dimethyl sulfoxide (DMSO) on the electrocardiogram (ECG) in freely moving male Balb/c mice. Gen Pharmacol 1995;26:1403–1407

22. Levitt HE, Cyphert TJ, Pascoe JL, et al. Glucose stimulates human beta cell replication in vivo in islets transplanted into NOD-severe combined immunodeficiency (SCID) mice. Diabetologia 2011;54:572–582

23. Diiorio P, Jurczyk A, Yang C, et al. Hyperglycemia-induced proliferation of adult human beta cells engrafted into spontaneously diabetic immunodeficient NOD-Rag1null IL2rγnull Ins2Akita mice. Pancreas 2011;40:1147–1149

24. Flier SN, Kulkarni RN, Kahn CR. Evidence for a circulating islet cell growth factor in insulin-resistant states. Proc Natl Acad Sci U S A 2001;98:7475–7480

25. Dhawan S, Georgia S, Tschen SI, Fan G, Bhushan A. Pancreatic β cell identity is maintained by DNA methylation-mediated repression of Arx. Dev Cell 2011;20:419–429

26. Dahl JA, Collas P. MicroChIP–a rapid micro chromatin immunoprecipitation assay for small cell samples and biopsies. Nucleic Acids Res 2008;36:e15

27. Carlson ME, Conboy MJ, Hsu M, et al. Relative roles of TGF-beta1 and Wnt in the systemic regulation and aging of satellite cell responses. Aging Cell 2009;8:676–689

28. Doyle KP, Cekanaviciute E, Mamer LE, Buckwalter MS. TGFβ signaling in the brain increases with aging and signals to astrocytes and innate immune cells in the weeks after stroke. J Neuroinflammation 2010;7:62

29. El-Gohary Y, Tulachan S, Wiersch J, et al. A Smad signaling network regulates islet cell proliferation. Diabetes 2014;63:224–236

30. Nomura M, Zhu HL, Wang L, Morinaga H, Takayanagi R, Teramoto N. SMAD2 disruption in mouse pancreatic beta cells leads to islet hyperplasia and impaired insulin secretion due to the attenuation of ATP-sensitive K+ channel activity. Diabetologia 2014;57:157–166

31. Simeone DM, Zhang L, Treutelaar MK, et al. Islet hypertrophy following pancreatic disruption of Smad4 signaling. Am J Physiol Endocrinol Metab 2006; 291:E1305–E1316

32. Smart NG, Apelqvist AA, Gu X, et al. Conditional expression of Smad7 in pancreatic beta cells disrupts TGF-beta signaling and induces reversible diabetes mellitus. PLoS Biol 2006;4:e39

33. Xiao X, Wiersch J, El-Gohary Y, et al. TGFβ receptor signaling is essential for inflammation-induced but not β-cell workload-induced β-cell proliferation. Diabetes 2013;62:1217–1226

34. Lin HM, Lee JH, Yadav H, et al. Transforming growth factor-beta/Smad3 signaling regulates insulin gene transcription and pancreatic islet beta-cell function. J Biol Chem 2009;284:12246–12257

35. Hannon GJ, Beach D. p15INK4B is a potential effector of TGF-beta-induced cell cycle arrest. Nature 1994;371:257–261

36. Reynisdóttir I, Polyak K, Iavarone A, Massagué J. Kip/Cip and Ink4 Cdk inhibitors cooperate to induce cell cycle arrest in response to TGF-beta. Genes Dev 1995;9:1831–1845

37. Tremain R, Marko M, Kinnimulki V, Ueno H, Bottinger E, Glick A. Defects in TGF-beta signaling overcome senescence of mouse keratinocytes expressing v-Ha-ras. Oncogene 2000;19:1698–1709

38. Padua D, Massagué J. Roles of TGFbeta in metastasis. Cell Res 2009;19: 89–102

39. Rane SG, Lee JH, Lin HM. Transforming growth factor-beta pathway: role in pancreas development and pancreatic disease. Cytokine Growth Factor Rev 2006;17:107–119

40. Tulachan SS, Tei E, Hembree M, et al. TGF-beta isoform signaling regulates secondary transition and mesenchymal-induced endocrine development in the embryonic mouse pancreas. Dev Biol 2007;305:508–521

41. Sjöholm A, Hellerström C. TGF-beta stimulates insulin secretion and blocks mitogenic response of pancreatic beta-cells to glucose. Am J Physiol 1991;260: C1046–C1051

42. Blum B, Roose A, Barrandon O, et al. Reversal of β cell de-differentiation by a small molecule inhibitor of the TGFβ pathway. ELife 2014;3:e02809

43. Cao R, Tsukada Y, Zhang Y. Role of Bmi-1 and Ring1A in H2A ubiquitylation and Hox gene silencing. Mol Cell 2005;20:845–854